

# Metal-Transfer-Micromolded RF Components for System-On-Package (SOP)

Yanzhu Zhao, Yong-Kyu Yoon, and Mark G. Allen

Microelectronics Research Center (MIRC), School of Electrical and Computer Engineering

Georgia Institute of Technology, Atlanta, GA 30332

Tel: (404)894-9909, Email: yzhao@gatech.edu

## Abstract

This paper reports a metal-transfer-micromolding (MTM) technique for simultaneous implementation of metallized high aspect ratio molded polymer RF passive components, as well as an organic RF circuit board, in a high performance and cost-effective fashion. A system on package (SOP) integration scheme of air lifted RF components can be realized by this process. Two test vehicles have been utilized to demonstrate the feasibility of the proposed process: planar coplanar waveguide (CPW)-based band stop filters and an air-lifted monopole antenna array, both operating in Ka-band. The measured filter characteristic shows a loss of less than 2.5 dB in passband and 20dB in stopband, which agrees well with HFSS10.0 simulations. The monopole antennas show good radiation performance and the 10dB bandwidths at the resonant radiation frequencies are as large as 21.5% for the tested structures.

## Introduction

Rapid growth in personal communication devices has motivated the development of high performance and low-cost RF passive components. Planar millimeter-wave components such as microstrip antennas or printed-circuit patch antennas are widely used due to their ease of manufacture, low cost, simple fabrication, and relative ease of integration with monolithic systems. However, those printed-circuit passive components can suffer from substrate dielectric loss, mutual coupling with their substrate, and surface wave perturbation issues [1]-[3]. Air-lifting (i.e., fabricating components with integral air gaps or other features to minimize substrate coupling) is a possible solution to the above problem. Components such as antennas, couplers, inductors, filters, or resonators may particularly benefit from air-lifting. Recently, a series of air-lifted RF components have been demonstrated using advanced surface-micromachining 3-D MEMS technologies including a polymer-core conductor technology [4]-[6], self-assembly using surface tension [7], an electroplating bonding technology [8], and a plate-up through-via-mold technology [9]. Often these processes rely on multiple deposition and LIGA lithographic steps potentially resulting in high fabrication cost and process complexity.

In SOP integration, multifunctional RF components should be implemented on a single substrate and package to realize the promise of a low cost, low loss and miniaturized microwave front-end module [10]. However, these air-lifted RF components usually have very different geometries and aspect ratios from each other. For example, monopole antennas are as high as quarter wavelength (order 1mm at W-band, and more than 2mm at Ka band), while an air-lifted coupler or inductor is usually at a height of hundreds of microns. Fig.1 shows a schematic example of multiple,

integrated air-lifted RF components with different profiles on the same substrate. This structural complexity may further increase the fabrication cost. Recently integration of air cavity resonators and monopole antennas has been demonstrated by stereolithography followed by a metal coating [11]. Although successful as a prototyping technology, this approach lacks the cost efficiency of batch fabrication, and the core materials set is limited to stereolithography-compatible resins. More batch-compatible approaches, such as conventional microelectromechanical systems (MEMS) technologies, are challenged by the fabrication of the multiheight and large-aspect-ratio structures of Fig.1. However, such structures can be achieved in a batch-compatible manner using micromolding technology.

Molding technology has been widely used in microelectronics packaging to physically protect integrated circuits and increase the long-term reliability of electronics [12]-[13]. Molding has advantages not only of low cost but also versatility of materials with desirable dielectric, mechanical and thermal properties [14]. For these reasons, micromolding (i.e., applying molding techniques to create parts with micron-scale features) has emerged as a promising fabrication technology. Fabrication costs of micromolded parts are almost independent of the complexity of the design, assuming a high enough volume that mold die costs can be amortized over many parts. The cost of the raw material in most cases is negligibly low, because only small material quantities are required for micro components. Therefore, parts fabricated by micromolding, even from high-end materials, are suitable for applications requiring extremely low-cost components. Further, although many polymers are lossy at RF frequencies, some polymers such as liquid crystal polymer (LCP) have excellent dielectric properties. It is also possible to tune the dielectric properties of polymers, for example by addition of appropriate powders such as ceramic or silver [15]. Additives and polymer material choice can also influence the mechanical properties of the molded structure, enabling structures ranging from soft and elastic to hard and brittle.

For SOP integration of different RF components, the transmission lines that interconnect these components are very important. However, it is difficult to pattern these interconnects for the molded components, especially when the molded components contain substantial three-dimensionality, due to incompatibility with standard metal patterning techniques such as photolithography, etching, or lift-off. Shadow masks used in metal film deposition can be a possible way to pattern metal films on molded structures, however it is very difficult to pattern both the RF air lifted components as large as several millimeters and the transmission line as narrow as tens of microns by a single shadow mask. A more accurate and simple metal patterning technique is required for molded 3-D components.

Recently there has been great interest in metal patterning techniques based on non-covalent adhesion, such as so-called ‘nano transfer printing’ (nTP) [16]. In this paper, the metal transfer mechanism is introduced into the molding process, creating a metal transfer micro-molding (MTM) fabrication approach. Both fully-metallized air-lifted RF components as well as metallized interconnects can be formed simultaneously by the MTM process. The technology is demonstrated through the fabrication of RF components such as Ka-band filters and monopole antennas.

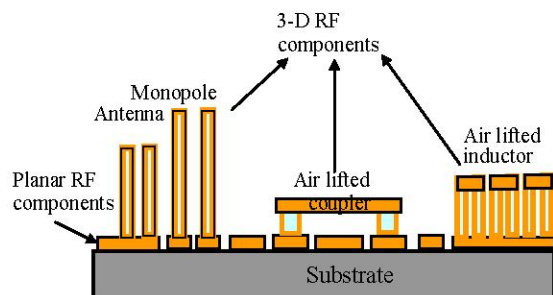


Fig. 1 Schematic drawing illustrating an example of integration of air-lifted RF components of differing functionalities and geometries on the same substrate

## Fabrication

A conventional micromolding process comprises three steps: master fabrication, mold preparation, and final part casting. In the MTM process, an additional step is introduced in which the metal is pre-patterned in the mold, and is transferred to the final part during the casting step. The MTM process is schematically illustrated in Figures 2-4 below.

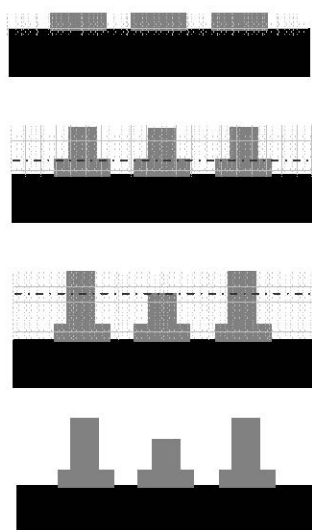


Fig. 2 Schematic of the master fabrication

**Master fabrication** A master device is initially fabricated and can be used repeatedly to generate multiple batches of molds and devices. There are many approaches to master realization, including conventional photolithography on either thick or thin resists, as well as stereolithography. A popular technique from the MEMS community is photolithography of negative photo-definable epoxy SU-8 to make high aspect ratio 3-D structures. A typical multilayer fabrication process is shown

in Fig. 2. A first layer of SU-8 is patterned to define the structure of the planar RF components such as the transmission line, which in this work, is a coplanar waveguide (CPW). Then several layers of SU-8 are patterned one by one to define the 3-D structures with differing height, such as a monopole antenna array at various resonant frequencies. After the multi exposure and bake steps, the structure can be finalized in one develop and cure step.

**Mold preparation** After the master is fabricated, a negative mold is created by casting and curing a suitable molding material, such as polydimethylsiloxane (PDMS), around the master. Commercially available Sylgard 184 prepolymer (Dow Corning) is used in this work. The mold is then separated from the master structure.

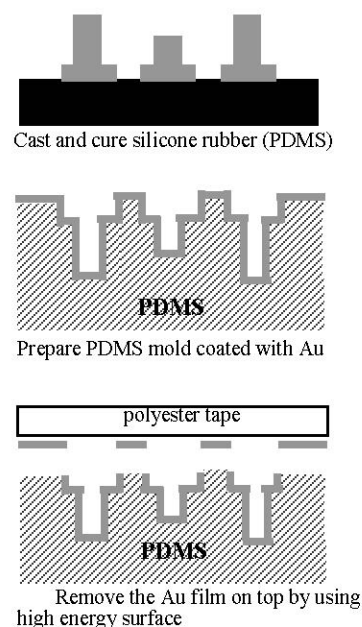


Fig 3. Schematic of the mold preparation, patterning, and metallization

**Mold metallization** The PDMS mold is coated with a thin metal film (usually 300nm–500nm Au or Ti/Au/Ti multilayer) by e-beam or DC sputter deposition. A transfer printing process is performed to remove the metal film on the raised regions of the stamp mold [16], by immediately placing the freshly metal-coated PDMS mold onto a flat, smooth substrate leads to “wetting” that provides intimate contact between the two surfaces. The substrate that we use is a standard polyester tape (Shercon™ PC21 masking tape) with a thin monolayer of adhesive. The polyester tape is gently peeled off and the metal layer on the raised region is transferred to the tape. Now the original PDMS mold has metal film coated only on the recessed regions that were originally patterned during the master fabrication step, and no subsequent patterning on three-dimensional surfaces is required.

**Metal Transfer Molding** Polymer (uncured, melted or dissolved in solvent) in the liquid state is cast into the PDMS

mold. Although standard injection molding approaches can be used in this step, for the polymers studied in this work only vacuum or heat was necessary to ensure full wetting of the PDMS mold by the polymer. Further, it was observed that the patterned metal film on the recessed regions of the mold aided wetting. After the cast polymer is solidified, the PDMS stamp mold is peeled off and the metal film within the recessed region is completely transferred to the molded part. The transferred metal is then optionally thickened using either electrodeposition or electroless deposition of appropriate metals.

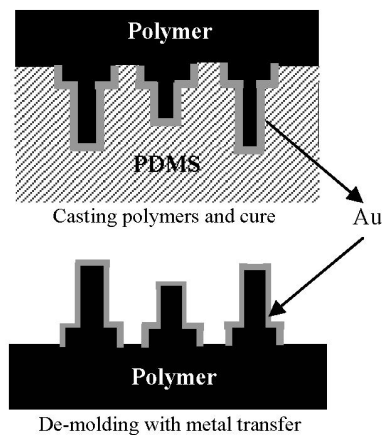


Fig. 4 Schematic of final step of metal transfer molding

Similar to nano-transfer printing (nTP) by noncovalent surface forces [16], the metal transfer mechanism here is also based on the different strengths of nonspecific adhesion between the PDMS-metal and polymer-metal interfaces. For most materials, the adhesion strength of the PDMS interface is weaker than that of the other interface, due primarily to the extremely low surface energy ( $19.8 \text{ mJ/m}^2$ ) of the PDMS.

Several polymers that are widely used in replica molding have been utilized for 3-D metal transfer demonstration: polymethyl methacrylate (PMMA) and polyurethane (PU); biodegradable polymers such as poly(L-lactic acid) (PLLA); photo-curable epoxy resin such as stereolithography apparatus (SLA) resin; and epoxy based negative photo resists such as SU-8. For the above materials, the metal films are completely transferred from PDMS, and the transferred gold film on the molded polymers shows similar adhesion strength with the directly deposited gold film based on Scotch™ tape adhesion tests.

Fig.5 displays a set of SEM and optical microscope images of an example of metal transfer molding. A molded array of micro posts is coated with gold film by metal transfer, and the posts are electrically interconnected in a diagonal pattern. The conductivity is also investigated by measurement using four probe station and the measurement is close to the theoretical simulations.

## Results

We exploit the application of 3-D metal transfer molding technique for the fabrication of low-cost, organic mm-wave components. Transmission lines are the basic interconnect

units of RF components, and in particular the coplanar waveguide (CPW) geometry is widely used in current RF modules, primarily because of its simple processing with no via holes as well as its capability of integration with active devices. The fabrication of CPW structures using metal transfer micromolding is investigated. Fig.6 shows a schematic view of the process. After removing the metal film on the raised surface of the PDMS mold by a polyester tape, the metal film on the bottom transfers to the molded polymers, where electrically isolated air gaps are uniquely formed. These air gaps reduce the substrate coupling and the subsequent loss. The simulated E-field distribution of the MTM-fabricated CPW is given in Fig.7(a), which shows the E-field is mainly confined between the edges of the metal lines. As a result, most of the substrate couplings occur in these E-field crowded regions. So it is most effective to reduce the substrate coupling and the subsequent loss by removing the substrate material in these regions [17]. By this molding process, a CPW with airgap can be directly fabricated. The simulated loss curves for a 10mm long CPW with or without air gap on epoxy are also shown in Fig.7(b). For example, on a high loss epoxy substrate with loss tangent of 0.06, the transmission power is 60% with airgap coupling while only 30% without airgap coupling.

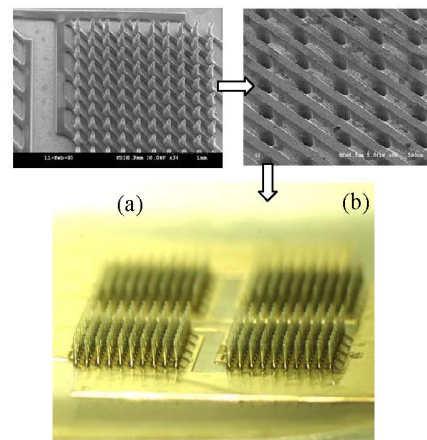


Fig.5 An array of electrodes ( $100 \mu\text{m}$  diameters) molded by photocurable epoxy resin. (a) master structure by SU-8 (b) PDMS mold (c) molded epoxy resin structure with transferred gold

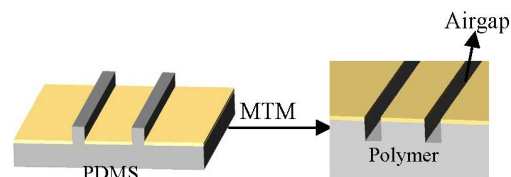


Fig.6 Schematic of molded CPW on polymers

The characteristic impedance of the waveguide is increased due to the airgap. Figure 8 shows a calculated impedance of CPW by standard lithography or molding of epoxy resin. The characteristic impedance has been calculated as a function of normalized center conductor width, using HFSS 10.0. The gap width and depth is fixed to  $50 \mu\text{m}$  for these curves in



order to maintain compatibility with both fabrication and measurement facilities. The ground plane is assumed to be infinite.

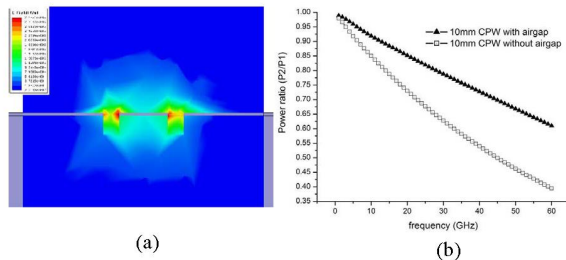


Fig.7 (a) The E-field distribution of an molded airgap CPW using HFSS10.0MTM (b) simulated transmission power of a CPW on a loss epoxy substrate.

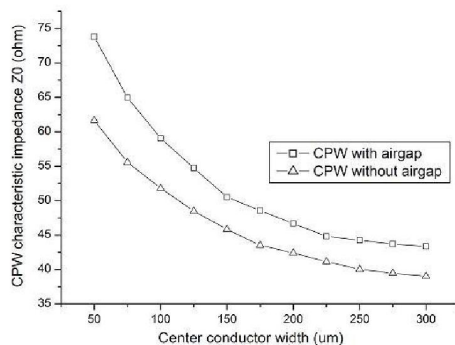


Fig.8 Impedance of CPW transmission line on epoxy resin with or without air gap

Based on these designs, a band-stop filter is demonstrated by the MTM process. This filter is designed based on the triple-folded CPW short stub resonator to minimize the size of the filter [18], and the stub length is  $\lambda/12$  at 30GHz with the width of each stub finger at  $50\mu\text{m}$ . Fig.9(a) shows the schematic of the filter design. A photomicrograph of the PDMS mold of the band-stop filter is shown in Fig.9(b), and the metal film on the raised region of the PDMS mold is removed by a polyester tape shown in 9(c). The fabricated filter is shown in 9(d), and 9(e) shows an array of filters made on a flexible substrate by MTM processes.

The characteristics of the MTM molded filters with  $35\mu\text{m}$  or  $25\mu\text{m}$  airgaps are given in Fig. 9(f)(g). An insertion loss ( $S_{21}$ ) of about  $-2.5\text{dB}$  at pass band is observed. The insertion loss in the stopband is approximately 20dB which is very close to the HFSS simulation. Results from the BPF demonstrate that planar components such as CPW transmission lines and stub filters can be successfully fabricated by this molding process. An integration of the CPW transmission line and high-aspect-ratio monopole antennas is further demonstrated.

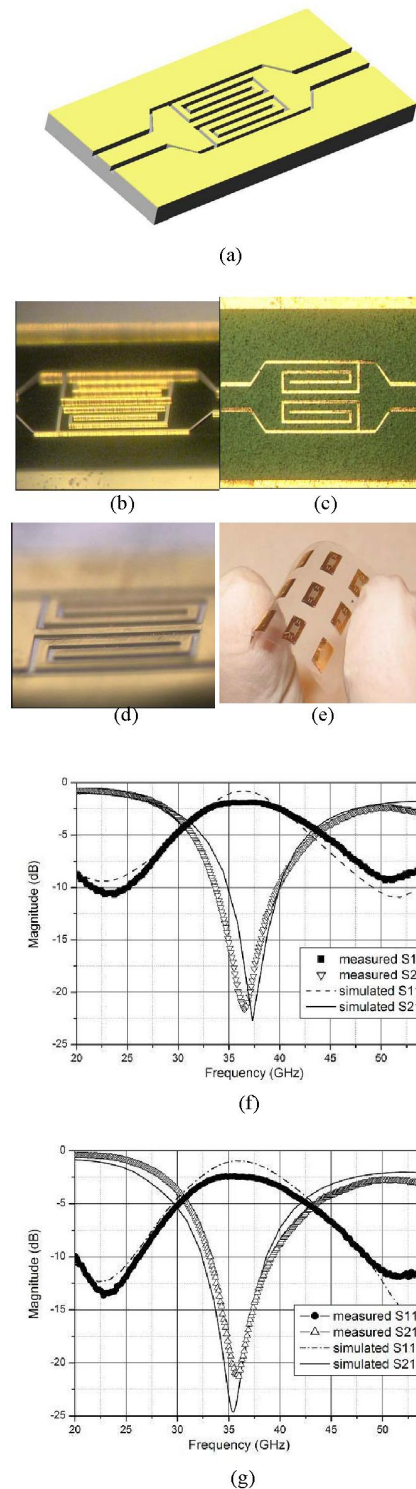


Fig.9 MTM molded band stop filter array and the characteristics

One of the key components for a wireless millimeter-wave system is its radiating structure, i.e., its antenna. Although wire antennas (e.g., dipole or monopole antennas) or cavity antennas can be considered as alternatives to printed-circuit patch antennas because of their broad bandwidth, low loss, and reduced dependence on substrate, fabrication difficulty has prevented them from being efficiently implemented and

integrated in a cost effective fashion. Using a molding process with metal transfer offers the advantages of substrate independence as well as ease of integration with other radiation structures at different resonant frequencies. An array of cylindrical quarter-wavelength monopole antennas fed by CPW on the same substrate operating in Ka-band is fabricated to demonstrate the simultaneous integration of 3-D and planar RF components by MTM. Both the monopoles and the substrate are made of molded epoxy resin with an aspect ratio up to 14:1.

In our design, the central operating frequency for the monopole is chosen in Ka-band (18-40GHz): 26GHz, 30GHz, 32GHz, and 42GHz. The feeding schematic is simply connecting the CPW line without other impedance transforming techniques which would not perturb the radiation pattern (Fig.10).

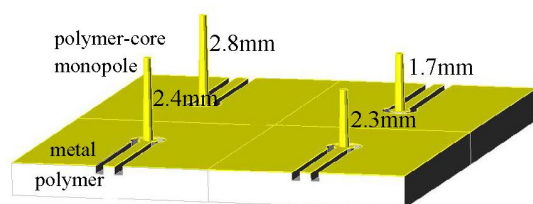
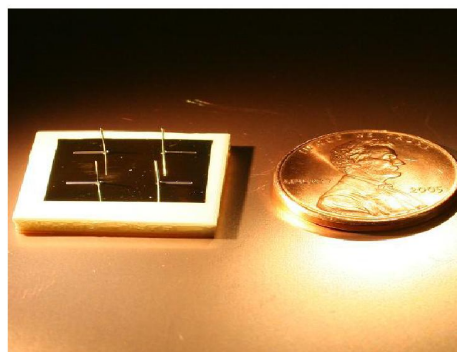


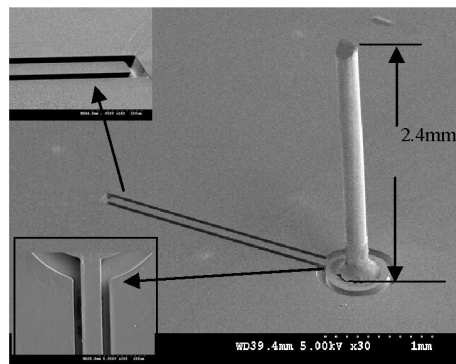
Fig.10 The schematic of a monopole antenna array operating in 26, 30, 32, 42GHz

The master structures are fabricated by stereolithography, and the molded structures are made by photo-curable epoxy resin (Accura® si100) which can be solidified by UV light ( $10\text{mW}/\text{cm}^2\text{second}$ ) within 1 minute after casting, and the metal is completely transferred during this short solidification period. All monopoles at the same diameter ( $200\text{ }\mu\text{m}$ ) and of different heights (1.7mm to 2.8mm) are molded on the same substrate. The fabricated device is shown in Fig.11. Since the aspect ratio is as high as up to 14: 1, an additional metal deposition step is needed to metallize the protruding portions of the monopoles by using a shadow masks. This step is only needed for high aspect ratio structures to achieve the conformal metal coatings on the sidewalls, while a precise pattern such as the CPW transmission line on the substrate have been achieved during the metal transfer molding process. The transferred and further deposited metal film work as a seed layer in the following electroplating process by which the final metal layer thickness is about  $10\text{ }\mu\text{m}$  (above 5 times the skin depth).

All the monopole pillars and the substrate are molded from the same material, so there is no mechanical interface between the substrate and the 3-D structures. Unlike the previous polymer core techniques using SU-8 on a glass or quartz substrate, there is no thermal expansion mismatch and delamination issues for the MTM molded RF devices.



(a)



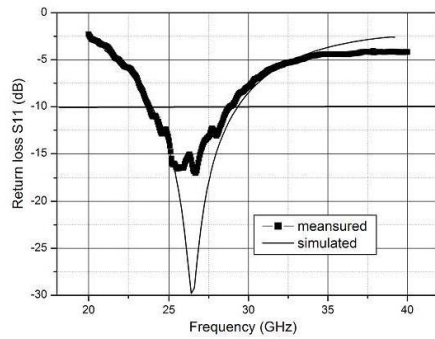
(b)

Fig.11 (a) a picture of a fabricated monopole antenna array operating at resonant frequencies from 25GHz to 42GHz. (b) a SEM picture of the monopole antenna with height of 2.4mm

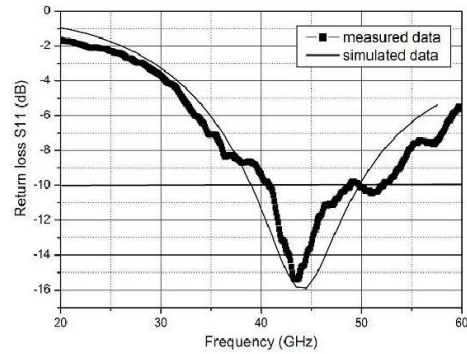
An S11 measurement is performed by an Agilent 8510X vector network analyzer as shown in Fig.12. Greater than 15 dB return loss bandwidth is achieved. The 10dB-bandwidths at the resonant radiation frequencies are 21.5%, 15.8%, 13.1%, and 18.4%, respectively, for the tested structures. The measurements show a good radiation performance at all the resonant radiation frequencies, and simulation by HFSS10.0 shows very close results to the measured resonant frequency and bandwidth. It demonstrates that this 3-D metal transfer molding process is very promising in the organic RF communication systems. The purpose of this structure is to illustrate the capability of metal transfer micromolding to create radiating structures for millimeter wave applications.

Molding processes, however, have limitations to certain structures, such as the re-entrant structures for air lifted dipole antenna or horn antenna, and self-close structures such as cavity resonators or air lifted inductors. A possible solution is to build the two counterpart structures by the MTM process and assembly them together to realize the re-entrant or self – close structures. The demonstration of SOA integration of these components will be done in future work.



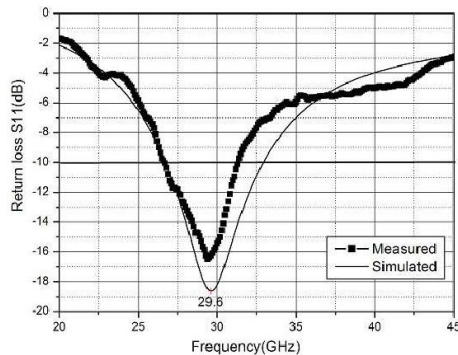


(a) Return loss of 2.83mm high monopole antenna

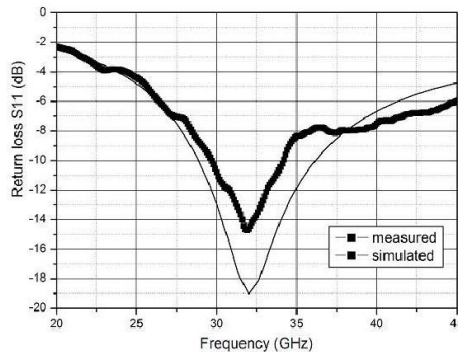


(d) Return loss of 1.71mm high monopole antenna

Fig.12 The measured and simulated return loss S11 of monopole antennas operating at different resonant frequencies from 25GHz to 43GHz (all antennas are in the same substrate and fed by CPW)



(b) Return loss of 2.43mm high monopole antenna



(c) Return loss of 2.34mm high monopole antenna

## Conclusion

This work introduces a metal transfer mechanism into the molding process, so-called metal transfer molding (MTM) process. This fabrication approach has been demonstrated by fabricating a planar bandstop filter and a monopole radiator array with good performance. It has great potentials in fabricating high performance organic RF devices in easy fabrication, low cost, and wide selection of materials and easily extended to integrate with other RF front-end components and to realize more high performance compact millimeter wave system on package (SOP).

## Acknowledgment

This work was supported in part by the Air Force Multidisciplinary University Research (MURI) Program under contract FA9550-05-1-0411. The authors would like to thank Bo Pan of the Georgia Electronic Design Center for assistance with measurements.

## References

1. David M. Pozar, "Considerations for Millimeter Wave Printed Antennas," *IEEE Trans. Antennas and Propagation*, vol. AP-31, no. 5, 1983, pp. 740-747
2. F. K. Schwering, "Millimeter wave antennas," *Proceedings of the IEEE*, vol. 80, no. 1, 1992, pp. 92-102
3. J. Papapolymerou, et al, "Micromachined Patch Antennas," *IEEE Trans. Antennas and Propagation*, Vol. 46, No. 2, 1998, pp. 275-283
4. Y.-K. Yoon, et al, "Polymer-Core Conductor Approaches for RF MEMS," *IEEE Journal of Microelectromechanical Systems (MEMS)*, vol. 14, no. 5, 2005, pp. 886-894
5. B. Pan, et al, "High Performance System-on-Package Integrated Yagi-Uda Antennas for W-band Applications and mm-Wave Ultra-Wideband Data Links", *Proceedings of 2006 ECTC*, San Diego, CA, May 31- Jun2, 2006
6. B.Pan, et al, "A High Performance Surface-Micromachined Elevated Patch Antenna", *Proceedings of*

- the 2005 IEEE-APS Symposium, pp.397-400, vol.1B, Washington, DC, July, 2005. pp1712-1717
7. G.W. Dahlmann, et al, "High Q Achieved in Microwave Inductors Fabricated by Parallel Self-Assembly," *Proceedings of International Conference on Solid-State Sensors and Actuators*, Munich, Germany, June 10-14, 2001, pp. 1098-1101.
  8. Y.-H. Joung, et al, "Integrated inductors in the chip-to-board interconnect layer fabricated using solderless electroplating bonding," *IEEE International Microwave Symposium*, Seattle, WA, USA, pp.1409-1412, 2002.
  9. Man-Lyun Ha, et al, "Q-band Micro-patch Antennas implemented on a High Resistivity Silicon substrate using the Surface Micromachining Technology", *Proc. of IEEE International Microwave Symposium*, June, 2004, pp.1189-1192
  10. R.R.Tummala, et al, "The SOP for Miniaturized, Mixed-Signal Computing, Communication and Consumer Systems of the Next Decade", *IEEE Transactions on Advanced Packaging*, Vol.27 No.2, pp.250-267, May 2004.
  11. Chappell, W.J, et al, "Applications of layer-by-layer polymer stereolithography for three-dimensional high-frequency components", *IEEE Transactions on microwave theory and techniques*, vol.52, Issue 11, 2004, pp.2567 – 2575
  12. C.P.Wong, et al, 'Recent Advances in Plastic Packaging of Flip-Chip and Multichip Modules (MCM) of Microelectronics', *IEEE Transactions on Components and Packaging Technology*, Vol. 22, No. 1, 1999, pp.21
  13. R. R. Tummala, et al, *Microelectronic Packaging, Handbook*. New York: Van Nostrand Reinhold, 1989.
  14. Hanemann T, et al, 'Current status of micromolding technology', *Polym. News*, 25 224–9, 2000
  15. C.P.Wong, et al, 'Development of novel silver nanoparticles/polymer composites as high K polymer matrix by in-situ photochemical method', *Proceedings of Electronic Components and Technology Conference*, 2006. Proceedings. 56th, pp6
  16. J. A. Rogers, et al, "Nanotransfer printing by use of noncovalent surface forces", *Applied Physics Letters*, 85, 5730 (2004)
  17. Leung, L.L.W., et al, "Characterization and attenuation mechanism of CMOS-compatible micromachined edge-suspended coplanar waveguides on low-resistivity silicon substrate" *IEEE transactions on Components, Packaging and Manufacturing Technology, Part B: Advanced Packaging*, Volume 29, Issue 3, Aug. 2006 PP.496 – 503
  18. Katehi, L.P. et al, "Miniature stub and filter designs using the microshield transmission line", *Microwave Symposium Digest, 1995, IEEE MTT-S International*, 16-20 May 1995 PP675 - 678 vol.2